Low Scale Seesaw Models for Low Scale $U(1)_{L_\mu - L_\tau}$ Symmetry

Takeshi Araki,[1] Kento Asai,[2] Joe Sato,[3] and Takashi Shimomura[4]

[1]*Learning Support Center, Kogakuin University, 2665-1 Nakano, Hachioji, 192-0015 Tokyo, Japan*
[2]*Department of Physics, University of Tokyo, Bunkyo-ku, Tokyo 133-0033, Japan*
[3]*Department of Physics, Saitama University, Shimo-Okubo 255, 338-y8570 Saitama Sakura-ku, Japan*
[4]*Faculty of Education, University of Miyazaki, 1-1 Gakuen-Kibanadai-Nishi, 889-2192 Miyazaki, Japan*

Abstract

We propose models for neutrino masses and mixing in the framework of low scale $U(1)_{L_\mu - L_\tau}$ gauge extension of the standard model. The models are designed to spontaneously break $U(1)_{L_\mu - L_\tau}$ so that the $U(1)_{L_\mu - L_\tau}$ gauge boson acquires an MeV scale mass, which is required to solve the long-standing problem of muon anomalous magnetic moment.

Keywords: symmetry, lepton, collider
DOI: 10.31526/ACP.NDM-2020.9

1. INTRODUCTION

The extension of the standard model (SM) is one of the highest priority issues in modern particle physics; various types of new physics models have been proposed in the literature. One interesting possibility is gauging the muon number minus the tau number, that is, the so-called $U(1)_{L_\mu - L_\tau}$ gauge extension [1, 2, 3]. This could be one of the most natural extensions of the SM since it is gauge anomaly free within the SM particle contents. Furthermore, it was recently found, in Ref. [4] (see also Refs. [5, 6]), that the $U(1)_{L_\mu - L_\tau}$ gauge boson, $Z_{\mu\tau}$, with an MeV scale mass can settle the long-standing discrepancy of muon anomalous magnetic moment ($g_\mu - 2$) [7, 8, 9, 10, 11, 12] without conflicting other experimental constraints. Then, this result motivated many authors to study low scale $U(1)_{L_\mu - L_\tau}$ extension of the SM in various contexts: for instance, it was found that an MeV scale $Z_{\mu\tau}$ can relax the tension between the late time and the early time determination of the Hubble constant [13], implications for the dark matter problem were studied in Refs. [14, 15, 16, 17], and the detectability of such a light $Z_{\mu\tau}$ was discussed in Refs. [18, 19, 20, 21, 22, 23, 24, 25]. Moreover, it was pointed out in Refs. [26, 27, 28, 29] that an MeV scale $Z_{\mu\tau}$ causes significant attenuation in the flux of high energy cosmic neutrinos and can explain the unexpected dip in the energy spectrum of high energy cosmic neutrinos reported by the IceCube Collaboration.

From a viewpoint of the lepton mixing, the $U(1)_{L_\mu - L_\tau}$ symmetry is well known to naturally explain the observed large atmospheric mixing angle [30, 31, 32]. However, it is also well known that the exact $U(1)_{L_\mu - L_\tau}$ symmetry forbids many of entries in the neutrino mass matrix, and as a result the solar and the reactor mixing angle are forced to be zero. In order to remedy such a situation, extra scalars are often introduced to spontaneously break $U(1)_{L_\mu - L_\tau}$ and to revive some of the entries forbidden by $U(1)_{L_\mu - L_\tau}$, which provides us with an opportunity to realize zero textures in the neutrino mass matrix and testability of the model. Especially, the type-C [33] two-zero texture or two-zero-minor structure is frequently obtained [34, 35, 36, 37, 38, 39, 40, 41, 42], and these structures were consistent with experiments at that time. However, in Ref. [42], it has been pointed out that the type-C two-zero-minor structure is now driven into a corner by the combined upper bound on the sum of neutrino masses placed by the Planck Collaboration: $\sum_i m_i < 0.12$ eV [43].

In this work, we improve the previous studies mentioned above and propose experimentally consistent models for $U(1)_{L_\mu - L_\tau}$ extension of the SM. For this purpose, we combine the inverse and the linear seesaw mechanism and succeed in realizing two types of one-zero textures [44, 45, 46, 47, 48, 49]. Both of the obtained textures prefer inverted neutrino mass ordering and are consistent with the Planck bound as well as the bounds from neutrino oscillation experiments. We calculate the effective mass of neutrinoless double beta decay as our prediction and find that it is testable in next generation experiments. In the models, extra scalars are introduced to spontaneously break $U(1)_{L_\mu - L_\tau}$ and to give an MeV scale mass to $Z_{\mu\tau}$ in order that the $g_\mu - 2$ problem and the dip in the IceCube data can simultaneously be solved. We show that some of the extra scalar bosons can have MeV scale masses and can attenuate the flux of high energy cosmic neutrinos, just as the $Z_{\mu\tau}$ does.

2. MODELS

We begin with $U(1)_{L_\mu - L_\tau}$ extension of the SM and introduce left- and right-handed SM gauge singlet fermions, N_L and N_R. Although it may be natural to introduce three generations of N_R and N_L and assign them $U(1)_{L_\mu - L_\tau}$ charges as

	$N_{R_e}, N_{R_{\mu(\tau)}}$	$N_{L_e}, N_{L_{\mu(\tau)}}$	H	Φ	S_L	$S_{\mu\tau}$
$U(1)_{L_\mu - L_\tau}$	$0, 1(-1)$	$0, 1(-1)$	0	0	0	1
$U(1)_L$	1	1	0	-2	-2	0

$(N_{R(L)_e},\ N_{R(L)_\mu},\ N_{R(L)_\tau}) = (0, 1, -1)$. Nevertheless, in this work, we introduce only two generations and aim at building a minimal model. In this case, the following two possibilities can be considered, and we refer to them as Model-A and Model-B:

$$\begin{aligned} &\text{Model} - \text{A} \ \ddagger \ (N_{R(L)_e},\ N_{R(L)_\mu}) = (0, 1), \\ &\text{Model} - \text{B} \ \ddagger \ (N_{R(L)_e},\ N_{R(L)_\tau}) = (0, -1). \end{aligned}$$

Note that we omit the case of $(N_{R(L)_\mu},\ N_{R(L)_\tau}) = (1, -1)$ because it results in a neutrino mass matrix of

$$m_\nu = \begin{pmatrix} 0 & 0 & 0 \\ 0 & 0 & m \\ 0 & m & 0 \end{pmatrix}, \tag{1}$$

which predicts unrealistic neutrino mass spectrum and mixing. Note also that the other combinations give rise to gauge anomalies, so we do not consider them in what follows.

In addition to the SM Higgs doublet, H, the scalar sector is also augmented with a new $SU(2)_W$ doublet scalar having hypercharge 1/2 ($Y = 1/2$), Φ, and two SM gauge singlet scalars, S_L and $S_{\mu\tau}$. Here, $S_{\mu\tau}$ breaks the $U(1)_{L_\mu - L_\tau}$ symmetry and gives an MeV scale mass to the $U(1)_{L_\mu - L_\tau}$ gauge boson, $Z_{\mu\tau}$, after developing a vacuum expectation value (VEV). As studied in Refs. [26, 29], the $g_\mu - 2$ problem and the dip in the IceCube data can simultaneously be solved with $M_{Z_{\mu\tau}} = 11$ MeV and $g_{\mu\tau} = 5 \times 10^{-4}$, where $M_{Z_{\mu\tau}}$ is a mass of $Z_{\mu\tau}$ and $g_{\mu\tau}$ is the gauge coupling constant of $U(1)_{L_\mu - L_\tau}$. We refer to these values in this work and require $S_{\mu\tau}$ to develop

$$\langle S_{\mu\tau} \rangle = \frac{M_{Z_{\mu\tau}}}{g_{\mu\tau}} \simeq 20\,\text{GeV}. \tag{2}$$

Furthermore, we introduce a global lepton number symmetry $U(1)_L$, which is explicitly broken in the scalar potential, see Sec. **??**. The gauge singlet scalar S_L and the $SU(2)_W$ doublet scalar Φ are introduced to spontaneously break $U(1)_L$ and to generate tiny masses for neutrinos. In Table 2, we summarize the particle contents and the charge assignments of the models.

3. NEUTRINO MASSES AND MIXING

After the scalars develop VEVs, neutrinos develops mass term with the following 7×7 neutrino mass matrix:

$$\mathcal{M}_\nu = \begin{pmatrix} 0 & m_D & m_N \\ (m_D)^T & m_{RR} & m_S \\ (m_N)^T & (m_S)^T & m_{LL} \end{pmatrix} \tag{3}$$

where they take the forms of

$$\begin{aligned} m_D &= \begin{pmatrix} m_d^{ee} & 0 \\ 0 & m_d^{\mu\mu} \\ 0 & 0 \end{pmatrix}, km_N = \begin{pmatrix} m_n^{ee} & 0 \\ 0 & 0 \\ 0 & m_n^{\tau\mu} \end{pmatrix}, \\ m_S &= \begin{pmatrix} m_s^{ee} & m_s^{e\mu} \\ m_s^{\mu e} & m_s^{\mu\mu} \end{pmatrix}, m_{LL} = \begin{pmatrix} m_L & 0 \\ 0 & 0 \end{pmatrix}, \\ m_{RR} &= \begin{pmatrix} m_R & 0 \\ 0 & 0 \end{pmatrix}, \end{aligned} \tag{4}$$

in the case of Model-A, and

$$\begin{aligned} m_D &= \begin{pmatrix} m_d^{ee} & 0 \\ 0 & 0 \\ 0 & m_d^{\tau\tau} \end{pmatrix}, m_N = \begin{pmatrix} m_n^{ee} & 0 \\ 0 & m_n^{\mu\tau} \\ 0 & 0 \end{pmatrix}, \\ m_S &= \begin{pmatrix} m_s^{ee} & m_s^{e\tau} \\ m_s^{\tau e} & m_s^{\tau\tau} \end{pmatrix}, m_{LL} = \begin{pmatrix} m_L & 0 \\ 0 & 0 \end{pmatrix}, \\ m_{RR} &= \begin{pmatrix} m_R & 0 \\ 0 & 0 \end{pmatrix}, \end{aligned} \tag{5}$$

in the case of Model-B. All the entries are given by the couplings of neutrino fields and vev of scalar fields.

With an appropreate mass ordering

$$m_S \gg m_D \gg m_N, m_{RR}, m_{LL} \;, \tag{6}$$

the active neutrino mass matrix is derived as

$$\begin{aligned} m_\nu &\simeq -m_N (m_S)^{-1} m_D^T - m_D (m_S^T)^{-1} m_N^T \\ &+ m_D (m_S^T)^{-1} m_{LL} (m_S)^{-1} m_D^T \;, \end{aligned} \tag{7}$$

We emphasize that the obtained mass matrix is twofold: the first two terms stem from the so-called linear seesaw mechanism, while the last term from the inverse seesaw one.

4. NUMERICAL CALCULATIONS

We here numerically diagonalize the active neutrino mass matrix and check its consistency with experiments. In the calculations, we place the 3σ constraints on the neutrino oscillation parameters obtained in Ref. [50]:

$$\begin{aligned} &\sin^2\theta_{12} = 0.275 - 0.350 \;\; (0.275 - 0.350), \\ &\sin^2\theta_{23} = 0.418 - 0.627 \;\; (0.423 - 0.629), \\ &\sin^2\theta_{13} = 0.02045 - 0.02439 \;\; (0.02068 - 0.02463), \\ &\Delta m^2_{21}/10^{-5} = 6.79 - 8.01 \;\; (6.79 - 8.01), \\ &\Delta m^2_{31}/10^{-3} = 2.427 - 2.625 \;\; (\Delta m^2_{23}/10^{-3} = 2.412 - 2.611), \\ &\delta = 125^\circ - 392^\circ \;\; (196^\circ - 360^\circ) \;, \end{aligned} \tag{8}$$

for normal (inverted) mass ordering. These values are acheived with appropreates inputs. Also we can suppress the mixings with extra neutrinos.

As can be seen, both the neutrino mass matrices contain one zero and thus we can predict two observables. In the following subsections, we calculate the effective mass of neutrinoless double beta decay, $\langle m_{ee}\rangle$, as a function of the sum of active neutrino masses, $\sum_i m_i$, and check the consistency with the current bounds:

$$\langle m_{ee}\rangle < 0.061 - 0.165 \text{ eV}, \tag{9}$$

from the KamLAND-Zen Collaboration [51], where the uncertainty comes from the nuclear matrix element calculation, and the combined upper bound

$$\sum_{i=1}^{3} m_i < 0.12 \text{ eV}, \tag{10}$$

from the Planck Collaboration [43].

4.1. *Inverted ordering*

Let us first investigate the inverted ordering case. Within Eq. (8) we vary the active neutrino mass matrix that is we vary input parameters. We vary these parameters randomly with flat probability distributions in each range. In Fig. 1, we plot $\langle m_{ee}\rangle$ as a function of $\sum_i m_i$ and find that there exist parameter regions (red crosses, $\times$) in which all the constraints can be satisfied for both Model-A and Model-B. Note that, in the figures, the density of points has no statistical meanings; it shows the difficulty of finding solutions. For instance, in the areas where the density is low, it is difficult to find solutions because relatively strong parameter tuning is necessary to satisfy Eq. (8) , especially the small squared-mass-differences. As a reference, we also show the current 3σ upper and lower bounds (solid curves), which are derived by calculating

$$\langle m_{ee}\rangle = |(c_{12}c_{13})^2 m_1 + (s_{12}c_{13})^2 m_2 e^{i\alpha_{21}} + (s_{13}e^{-i\delta})^2 m_3 e^{i\alpha_{31}}|, \tag{11}$$

with Eq. (8) while varying the Majorana phases within $0 - 2\pi$. Also, full parameter regions of the models (dashed curves) are shown by solving the condition $(m_\nu)_{\tau\tau} = 0$:

$$\begin{aligned} &(s_{12}s_{23} - c_{12}c_{23}s_{13}e^{i\delta})^2 m_1 + (c_{12}s_{23} + s_{12}c_{23}s_{13}e^{i\delta})^2 m_2 e^{i\alpha_{21}} \\ &+(c_{23}c_{13})^2 m_3 e^{i\alpha_{31}} = 0, \end{aligned} \tag{12}$$

for Model-A, and $(m_\nu)_{\mu\mu} = 0$:

$$\begin{aligned} &(s_{12}c_{23} + c_{12}s_{23}s_{13}e^{i\delta})^2 m_1 + (c_{12}c_{23} - s_{12}s_{23}s_{13}e^{i\delta})^2 m_2 e^{\alpha_{21}} \\ &+(s_{23}c_{13})^2 m_3 e^{\alpha_{31}} = 0, \end{aligned} \tag{13}$$

for Model-B. Unfortunately, the current sensitivity on $\langle m_{ee}\rangle$ is not enough to test the predicted regions. However, in next generation experiments, the sensitivity is hoped to reach $\langle m_{ee}\rangle = \mathcal{O}(0.01)$ eV [52], so our models would be tested in the near future.

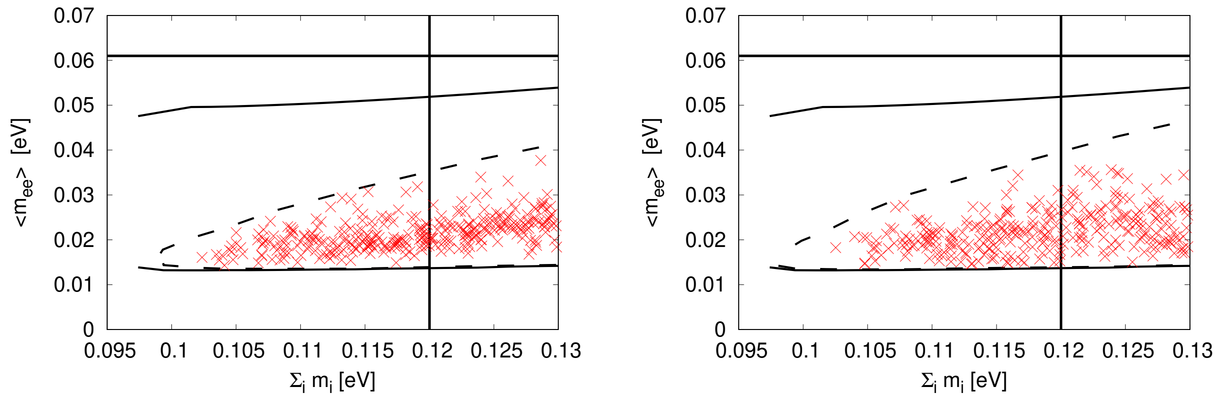

FIGURE 1: The effective mass of neutrinoless double beta decay, $\langle m_{ee} \rangle$, as a function of the sum of active neutrino masses, $\sum_i m_i$, in the case of inverted mass ordering, for Model-A (left panel) and Model-B (right panel). The solid curves display 3σ upper and lower bounds corresponding to Eq. (8). The regions surrounded by the dashed curves are full parameter regions of the models The horizontal solid lines indicate the tightest upper bound of Eq. (9), and the vertical lines indicate Eq. (10).

4.2. Normal ordering

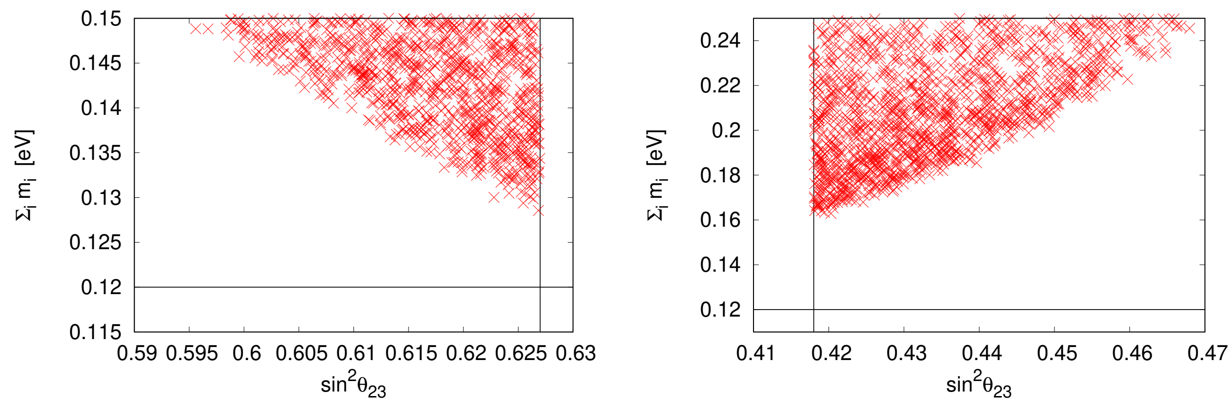

FIGURE 2: The sum of active neutrino masses, $\sum_i m_i$, as a function of $\sin^2\theta_{23}$ in the case of normal mass ordering, for Model-A (left panel) and Model-B (right panel). The horizontal solid lines correspond to Eq. (10), while the vertical lines are $\sin^2\theta_{23} = 0.627$ (left panel) and $\sin^2\theta_{23} = 0.418$ (right panel) which are the upper and the lower bound in Eq. (8), respectively.

For normal mass ordering, we find that both of the one-zero textures are now excluded by the Planck bound. In order to show this conclusion, we calculate $\sum_i m_i$ by solving Eqs. (12) and (13) and check their consistency. In Fig. 2, we show $\sum_i m_i$ as a function of $\sin^2\theta_{23}$ for the cases of $(m_\nu)_{\tau\tau} = 0$ (left panel) and $(m_\nu)_{\mu\mu} = 0$ (right panel). The neutrino oscillation parameters are randomly scattered within the 3σ ranges given in Eq. (8), while the Majorana phases are varied within $0 - 2\pi$.

5. NEUTRINO SECRET INTERACTIONS

Lastly, we briefly comment on the so-called neutrino secret interactions. Soon after the discovery of high energy cosmic neutrino events in the energy range between $\mathcal{O}(100)$ TeV and $\mathcal{O}(1)$ PeV by the IceCube Collaboration [53, 54], several authors pointed out that if there exist new light bosons having interactions with neutrinos, they could cause significant attenuation in the flux of high energy cosmic neutrinos by mediating resonant scattering with cosmic neutrino background [55, 56, 57, 26, 27, 28, 29]. Interestingly, one can indeed find a possible dip in the energy spectrum of high energy cosmic neutrinos around 400 TeV $-$ 1 PeV in the IceCube data, see Ref. [58] for the recent analysis. In our models, we have three candidates for such light bosons, that is, the CP-even neutral scalar h_3 and the CP-odd one ζ_3, as well as $Z_{\mu\tau}$. The detailed analysis for $Z_{\mu\tau}$ was already done in Refs. [26, 29]. Thus, in this section, we focus only on h_3 and ζ_3 and check whether they can serve as the mediator of the resonant scattering, just as $Z_{\mu\tau}$ does.

Suppose the light boson is scalar and has Yukawa interactions with active neutrinos, the interaction can be formulated as

$$g_\nu \bar{\nu} \nu^c \chi + h.c. \,. \tag{14}$$

According to Ref. [29], in order for the scalar χ to significantly attenuate the cosmic neutrino flux in the PeV region, its mass and the coupling constant should satisfy

$$M_\chi = \mathcal{O}(1-10)\ \text{MeV},\ \ g_\nu > \mathcal{O}(10^{-4})\ . \tag{15}$$

As shown in Sec. **??**, both h_3 and ζ_3 can have an MeV scale mass by suitably tuning the $U(1)_L$ breaking parameters B^2. As for the Yukawa coupling g_ν, in our models, it arises from the third term in Eq. (**??**), through the mixing in Eqs. (**??**) and (**??**). In the case of h_3, it arises as

$$y_N \overline{\nu_L}(N_L)^c \phi \to -y_N \left[\left(1-\frac{1}{2}\eta\eta^\dagger\right)\eta^T R\right]\bar{\nu}\nu^c h_3 \equiv g_\nu \bar{\nu}\nu^c h_3, \tag{16}$$

while for ζ_3, it is described as

$$iy_N \overline{\nu_L}(N_L)^c \xi \to -iy_N \left[\left(1-\frac{1}{2}\eta\eta^\dagger\right)\eta^T R\left(1-\frac{1}{2}r^2\right)\right]\bar{\nu}\nu^c \zeta_3 \equiv g'_\nu \bar{\nu}\nu^c \zeta_3. \tag{17}$$

Given our parameter setting: $\eta = \mathcal{O}(10^{-2})$, $R = v_\Phi/v_L = \mathcal{O}(10^{-1})$, and $r = v_\Phi/v_{\text{ew}} = \mathcal{O}(10^{-10})$, one obtains $g_\nu^{(\prime)} = \mathcal{O}(10^{-3})$, which is presumably large enough to attenuate the cosmic neutrino flux. A more detailed study will be done elsewhere.

6. SUMMARY

In summary, we propose models for an MeV scale $U(1)_{L_\mu - L_\tau}$ gauge boson, $Z_{\mu\tau}$, which is anticipated to exist to resolve the $g_\mu - 2$ problem as well as the possible dip in the energy spectrum of high energy cosmic neutrinos. We introduce extra scalars to spontaneously break $U(1)_{L_\mu - L_\tau}$ and to generate an MeV scale mass to $Z_{\mu\tau}$. Tiny neutrino masses and mixing are obtained by simultaneously invoking the linear and the inverse seesaw mechanism. Depending on the $U(1)_{L_\mu - L_\tau}$ charge assignment, the active neutrino mass matrix enjoys two types of one-zero textures, which endows the models with predictive power. Both of the textures prefer inverted neutrino mass ordering and would be tested in next generation experiments of neutrinoless double beta decay. Furthermore, we find that two of the extra scalars can acquire MeV scale masses while having interactions with active neutrinos. We briefly confirm that they can serve as the mediator of resonant scattering between high energy cosmic neutrinos and cosmic neutrino background, and that they could help us understand the existence of the unexpected dip in the IceCube data.

Finally, we comment on kinetic mixing between $U(1)_{L_\mu - L_\tau}$ and the SM electromagnetic $U(1)_{\text{em}}$ gauge symmetry. In our framework, we do not introduce the kinetic mixing term at the tree level, but it appears at the one loop level. In Refs. [20, 29], we studied implications of the loop-induced kinetic mixing for solar neutrino measurements and the detectability of $Z_{\mu\tau}$ at e^+e^- colliders. In contrast to the previous work, we here introduce extra fermions and scalars charged under $U(1)_{L_\mu - L_\tau}$. Nevertheless, there are no mass eigenstates that are charged under both $U(1)_{L_\mu - L_\tau}$ and $U(1)_{\text{em}}$, except for the SM mu and tau leptons. Hence, we expect that the same kinetic mixing as those in Refs. [20, 29] will also be obtained for the framework proposed in this paper.

ACKNOWLEDGEMENTS

This work was supported by JSPS KAKENHI Grants No. JP18H01210 (T.A., J.S., T.S.), No. JP19J13812 (K.A.), No. JP18K03651 (T.S.), and MEXT KAKENHI Grant No. JP18H05543 (J.S., T.S.).

References

[1] Robert Foot. New Physics From Electric Charge Quantization? *Mod.Phys.Lett.*, A6:527–530, 1991.
[2] X.G. He, Girish C. Joshi, H. Lew, and R.R. Volkas. NEW Z-prime PHENOMENOLOGY. *Phys.Rev.*, D43:22–24, 1991.
[3] Robert Foot, X. G. He, H. Lew, and R. R. Volkas. Model for a light Z-prime boson. *Phys. Rev.*, D50:4571–4580, 1994.
[4] Wolfgang Altmannshofer, Stefania Gori, Maxim Pospelov, and Itay Yavin. Neutrino Trident Production: A Powerful Probe of New Physics with Neutrino Beams. *Phys. Rev. Lett.*, 113:091801, 2014.
[5] S. N. Gninenko and N. V. Krasnikov. The Muon anomalous magnetic moment and a new light gauge boson. *Phys. Lett.*, B513:119, 2001.
[6] Seungwon Baek, N. G. Deshpande, X. G. He, and P. Ko. Muon anomalous g-2 and gauged L(muon) - L(tau) models. *Phys. Rev.*, D64:055006, 2001.
[7] G.W. Bennett et al. Final Report of the Muon E821 Anomalous Magnetic Moment Measurement at BNL. *Phys.Rev.*, D73:072003, 2006.
[8] Kirill Melnikov and Arkady Vainshtein. Hadronic light-by-light scattering contribution to the muon anomalous magnetic moment revisited. *Phys. Rev.*, D70:113006, 2004.
[9] Michel Davier, Andreas Hoecker, Bogdan Malaescu, and Zhiqing Zhang. Reevaluation of the Hadronic Contributions to the Muon g-2 and to alpha(MZ). *Eur. Phys. J.*, C71:1515, 2011. [Erratum: Eur. Phys. J. **C72**, 1874 (2012)].
[10] Kaoru Hagiwara, Ruofan Liao, Alan D. Martin, Daisuke Nomura, and Thomas Teubner. $(g-2)_\mu$ and alpha(M_Z^2) re-evaluated using new precise data. *J.Phys.*, G38:085003, 2011.
[11] Tatsumi Aoyama, Masashi Hayakawa, Toichiro Kinoshita, and Makiko Nio. Complete Tenth-Order QED Contribution to the Muon g-2. *Phys. Rev. Lett.*, 109:111808, 2012.

[12] Alexander Kurz, Tao Liu, Peter Marquard, and Matthias Steinhauser. Hadronic contribution to the muon anomalous magnetic moment to next-to-next-to-leading order. *Phys. Lett.*, B734:144–147, 2014.

[13] Miguel Escudero, Dan Hooper, Gordan Krnjaic, and Mathias Pierre. Cosmology with A Very Light $L_\mu - L_\tau$ Gauge Boson. *JHEP*, 03:071, 2019.

[14] Seungwon Baek. Dark matter and muon $(g-2)$ in local $U(1)_{L_\mu - L_\tau}$-extended Ma Model. *Phys. Lett.*, B756:1–5, 2016.

[15] Anirban Biswas, Sandhya Choubey, and Sarif Khan. FIMP and Muon $(g-2)$ in a $\mathrm{U}(1)_{L_\mu - L_\tau}$ Model. *JHEP*, 02:123, 2017.

[16] Ayuki Kamada, Kunio Kaneta, Keisuke Yanagi, and Hai-Bo Yu. Self-interacting dark matter and muon $g-2$ in a gauged $\mathrm{U}(1)_{L_\mu - L_\tau}$ model. *JHEP*, 06:117, 2018.

[17] Patrick Foldenauer. Light dark matter in a gauged $U(1)_{L_\mu - L_\tau}$ model. *Phys. Rev.*, D99(3):035007, 2019.

[18] S. N. Gninenko, N. V. Krasnikov, and V. A. Matveev. Muon g-2 and searches for a new leptophobic sub-GeV dark boson in a missing-energy experiment at CERN. *Phys. Rev.*, D91:095015, 2015.

[19] Yuya Kaneta and Takashi Shimomura. On the possibility of a search for the $L_\mu - L_\tau$ gauge boson at Belle-II and neutrino beam experiments. *PTEP*, 2017(5):053B04, 2017.

[20] Takeshi Araki, Shihori Hoshino, Toshihiko Ota, Joe Sato, and Takashi Shimomura. Detecting the $L_\mu - L_\tau$ gauge boson at Belle II. *Phys. Rev.*, D95(5):055006, 2017.

[21] Chuan-Hung Chen and Takaaki Nomura. $L_\mu - L_\tau$ gauge-boson production from lepton flavor violating τ decays at Belle II. D96(9):095023, 2017.

[22] S. N. Gninenko and N. V. Krasnikov. Probing the muon $g_\mu - 2$ anomaly, $L_\mu - L_\tau$ gauge boson and Dark Matter in dark photon experiments. *Phys. Lett.*, B783:24–28, 2018.

[23] Eung Jin Chun, Arindam Das, Jinsu Kim, and Jongkuk Kim. Searching for flavored gauge bosons. *JHEP*, 02:093, 2019. [erratum: JHEP07,024(2019)].

[24] Takaaki Nomura and Takashi Shimomura. Searching for scalar boson decaying into light Z' boson at collider experiments in $U(1)_{L_\mu - L_\tau}$ model. *Eur. Phys. J.*, C79(7):594, 2019.

[25] Yongsoo Jho, Youngjoon Kwon, Seong Chan Park, and Po-Yan Tseng. Search for muon-philic new light gauge boson at Belle II. 2019.

[26] Takeshi Araki, Fumihiro Kaneko, Yasufumi Konishi, Toshihiko Ota, Joe Sato, and Takashi Shimomura. Cosmic neutrino spectrum and the muon anomalous magnetic moment in the gauged $L_\mu - L_\tau$ model. *Phys.Rev.*, D91(3):037301, 2015.

[27] Ayuki Kamada and Hai-Bo Yu. Coherent Propagation of PeV Neutrinos and the Dip in the Neutrino Spectrum at IceCube. *Phys. Rev.*, D92(11):113004, 2015.

[28] Anthony DiFranzo and Dan Hooper. Searching for MeV-Scale Gauge Bosons with IceCube. *Phys. Rev.*, D92(9):095007, 2015.

[29] Takeshi Araki, Fumihiro Kaneko, Toshihiko Ota, Joe Sato, and Takashi Shimomura. MeV scale leptonic force for cosmic neutrino spectrum and muon anomalous magnetic moment. *Phys. Rev.*, D93(1):013014, 2016.

[30] Ernest Ma, D. P. Roy, and Sourov Roy. Gauged L(mu) - L(tau) with large muon anomalous magnetic moment and the bimaximal mixing of neutrinos. *Phys. Lett.*, B525:101–106, 2002.

[31] Sandhya Choubey and Werner Rodejohann. A Flavor symmetry for quasi-degenerate neutrinos: L(mu) - L(tau). *Eur.Phys.J.*, C40:259–268, 2005.

[32] Toshihiko Ota and Werner Rodejohann. Breaking of L(mu) - L(tau) Flavor Symmetry, Lepton Flavor Violation and Leptogenesis. *Phys.Lett.*, B639:322–331, 2006.

[33] Paul H. Frampton, Sheldon L. Glashow, and Danny Marfatia. Zeroes of the neutrino mass matrix. *Phys. Lett.*, B536:79–82, 2002.

[34] Julian Heeck and Werner Rodejohann. Gauged $L_\mu - L_\tau$ Symmetry at the Electroweak Scale. *Phys.Rev.*, D84:075007, 2011.

[35] Abhish Dev. Gauged L_μ-L_τ Model with an Inverse Seesaw Mechanism for Neutrino Masses. 2017.

[36] Takaaki Nomura and Hiroshi Okada. Zee-Babu type model with $U(1)_{L_\mu - L_\tau}$ gauge symmetry. *Phys. Rev.*, D97(9):095023, 2018.

[37] Takeshi Araki, Julian Heeck, and Jisuke Kubo. Vanishing Minors in the Neutrino Mass Matrix from Abelian Gauge Symmetries. *JHEP*, 07:083, 2012.

[38] Anirban Biswas, Sandhya Choubey, and Sarif Khan. Neutrino Mass, Dark Matter and Anomalous Magnetic Moment of Muon in a $U(1)_{L_\mu - L_\tau}$ Model. *JHEP*, 09:147, 2016.

[39] Kento Asai, Koichi Hamaguchi, and Natsumi Nagata. Predictions for the neutrino parameters in the minimal gauged $\mathrm{U}(1)_{L_\mu - L_\tau}$ model. *Eur. Phys. J.*, C77(11):763, 2017.

[40] Cheng-Wei Chiang and Koji Tsumura. Model with a gauged lepton flavor SU(2) symmetry. *JHEP*, 05:069, 2018.

[41] Takaaki Nomura and Hiroshi Okada. Neutrino mass generation with large $SU(2)_L$ multiplets under local $U(1)_{L_\mu - L_\tau}$ symmetry. *Phys. Lett.*, B783:381–386, 2018.

[42] Kento Asai, Koichi Hamaguchi, Natsumi Nagata, Shih-Yen Tseng, and Koji Tsumura. Minimal Gauged $\mathrm{U}(1)_{L_\alpha - L_\beta}$ Models Driven into a Corner. *Phys. Rev.*, D99(5):055029, 2019.

[43] N. Aghanim et al. Planck 2018 results. VI. Cosmological parameters. 2018.

[44] Zhi-zhong Xing. Implications of generalized Frampton-Glashow-Yanagida ansaetze on neutrino masses and lepton flavor mixing. *Phys. Rev.*, D69:013006, 2004.

[45] Alexander Merle and Werner Rodejohann. The Elements of the neutrino mass matrix: Allowed ranges and implications of texture zeros. *Phys. Rev.*, D73:073012, 2006.

[46] E. I. Lashin and N. Chamoun. The One-zero Textures of Majorana Neutrino Mass Matrix and Current Experimental Tests. *Phys. Rev.*, D85:113011, 2012.

[47] K. N. Deepthi, Srinu Gollu, and R. Mohanta. Neutrino mixing matrices with relatively large θ_{13} and with texture one-zero. *Eur. Phys. J.*, C72:1888, 2012.

[48] Radha Raman Gautam, Madan Singh, and Manmohan Gupta. Neutrino mass matrices with one texture zero and a vanishing neutrino mass. *Phys. Rev.*, D92(1):013006, 2015.

[49] Teruyuki Kitabayashi. Scotogenic dark matter and single-zero textures of the neutrino mass matrix. *Phys. Rev.*, D98(8):083011, 2018.

[50] Ivan Esteban, M. C. Gonzalez-Garcia, Alvaro Hernandez-Cabezudo, Michele Maltoni, and Thomas Schwetz. Global analysis of three-flavour neutrino oscillations: synergies and tensions in the determination of θ_23, δ_CP, and the mass ordering. *JHEP*, 01:106, 2019.

[51] A. Gando et al. Search for Majorana Neutrinos near the Inverted Mass Hierarchy Region with KamLAND-Zen. *Phys. Rev. Lett.*, 117(8):082503, 2016. [Addendum: Phys. Rev. Lett.117,no.10,109903(2016)].

[52] Neutrino 2018. https://www.mpi-hd.mpg.de/nu2018/, 2018.

[53] M. G. Aartsen et al. First observation of PeV-energy neutrinos with IceCube. *Phys. Rev. Lett.*, 111:021103, 2013.

[54] M. G. Aartsen et al. Evidence for High-Energy Extraterrestrial Neutrinos at the IceCube Detector. *Science*, 342:1242856, 2013.

[55] Kunihto Ioka and Kohta Murase. IceCube PeV–EeV neutrinos and secret interactions of neutrinos. *PTEP*, 2014(6):061E01, 2014.

[56] Kenny C. Y. Ng and John F. Beacom. Cosmic neutrino cascades from secret neutrino interactions. *Phys. Rev.*, D90(6):065035, 2014. [Erratum: Phys. Rev.D90,no.8,089904(2014)].

[57] Masahiro Ibe and Kunio Kaneta. Cosmic neutrino background absorption line in the neutrino spectrum at IceCube. *Phys. Rev.*, D90(5):053011, 2014.

[58] Claudio Kopper. Observation of Astrophysical Neutrinos in Six Years of IceCube Data. *PoS*, ICRC2017:981, 2018.